ON LIMIT SEISMIC FACTOR IN NONHOMOGENEOUS, ANISOTROPIC SLOPES

BY

Tomoyuki SAWADA*, Sumio G. NOMACHI**
and Wai F. CHEN***
(Received November 30, 1983)

SYNOPSIS

Sudden ground movement during earthquake induce large inertia forces in slopes. As a consequence, the inertia forces moving away from the slope tend to reduce the stability of the slope.

In this paper, it is attempted to evaluate the yield acceleration and the correspondig failure mechanism in a slope of anisotropic and nonhomogeneous soil by means of the upper bound techniques of pseudostatic limit analysis.

The term "anisotropic" means anisotropic cohesion strength and "nonhomogeneous", linearly varying cohesion strength in the direction of depth. The method of limit analysis is derived from the assumption that soil deformation obeys the flow rule associated with the Coulomb yield condition and volume increases as a plastic shearing deformation takes place.

Another assumption that soil mass slides with the angle Φ between the velocity vector and the slip surface like a rigid body, governs motion of the soil mass. Thus, obtained optimize solutions by "reduced gradient method" are good tendency. Also some results are compared with the ones caluculated by previous investigators to be in good agreement.

I. INTRODUCTION

Herein, the term "Nonhomogeneous soil" means only the cohesion strength, c which is assumed to vary linearly with depth (Fig. 1(c)). Figure 2 summarizes diagrammatically some of the simple cutting in normally consolidated clays with several forms of cohesion strength distribution being considered previously by several investigators. (Lo, 1965, Odenstad, 1963, Reddy and Srinivason, 1967, Taylor, 1948).

The term "Anisotropic soil" implies here the variation of the cohesion strength, c, with direction at a particular point. The anisotropy with respect to cohesion strength, c of the soil has been studied by several investigators. (Lo, 1965, Odenstad, 1963, Reddy and Srinivason, 1967, Taylor, 1948). It is found that the variation of cohesion strength, c, with direction approximates to the curve shown in Fig. 1 (b). In this paper, the variation of the apparent friction angle ϕ is not considered with respect

* Dept. of Civil Engineering Assoc. Professor
** Hokkaido UNIVERSITY
Dept. of Civil Engineering Professor
*** Purdue UNIVERSITY
Dept. of Civil Engineering Professor & Head of Structural Engrg.

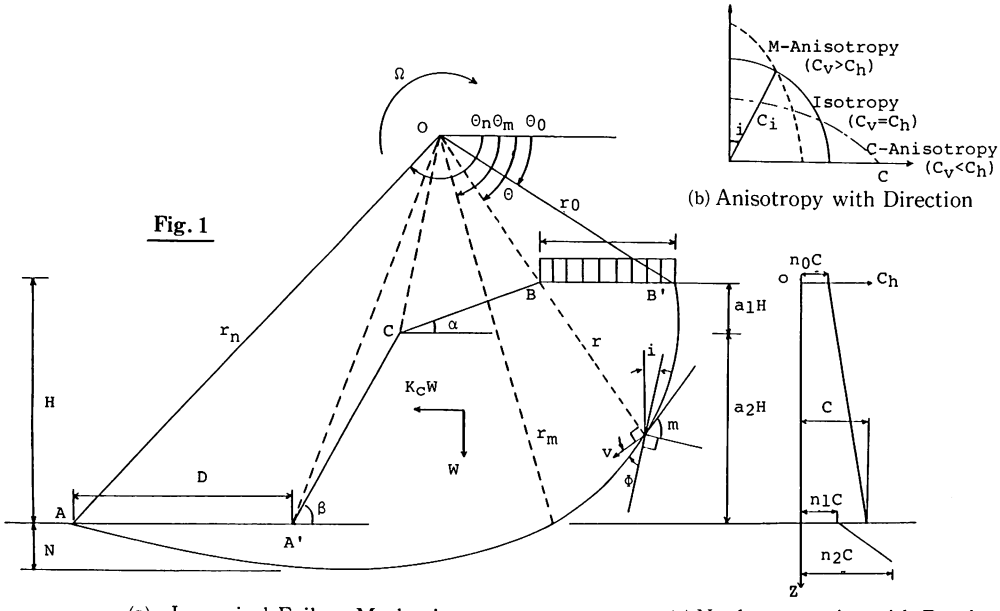

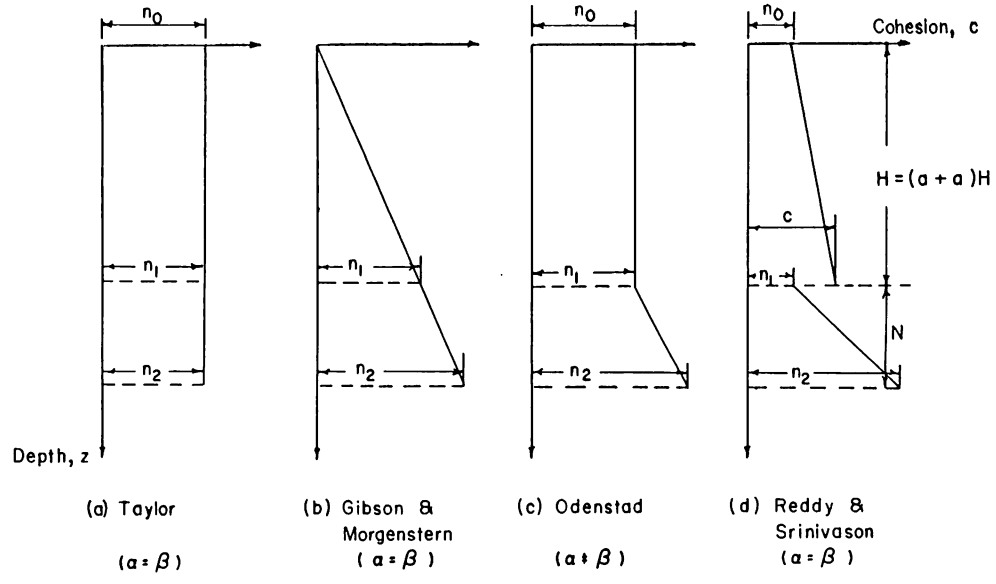

Fig. 2 Some Types of Linear Variasions of Cohesion With Depth

to either the nonhomogeneity or the anisotropy. In the following we assume that the cohesion strength c_i, with its major principal stress inclined at an angle i with the vertical direction, is given by

$$c_i = c_h + (C_v - c_h)\cos^2 i \qquad (1)$$

where c_h and c_v are the cohesion strength in the horizontal and vertical directions, respectively. The cohesion strengths may be termed as "principal cohesion strengths". (Lo, 1965) For example, the vertical cohesion strength, c_v can be obtained by taking vertical soil samples at any position and being investigated with the major principal stress applied in the same direction. The ratio of the principal cohesion strength c_h/c_v, denoted by k, is assumed to be the same at all points in the medium. $c_i = c_h =$

c_v or $k=1.0$ means an isotropic material. In Fig. 1 (a), the angle m is the angle between the failure plane and the plane which is normal to the direction of the major principle cohesion strength kept at an angle i with the vertical direction. This angle, according to Lo's test (1965), is found to be independent of the angle of rotation of the major principal stress.

II. GENERAL EXPRESSIONS

The geometrical relation L/r_o, H/r_o and N/r_o in Fig. 1 (a) can be expressed in the forms.

$$\frac{L}{r_o}=\cos\theta_o-\cos\theta_h\exp[(\theta_h-\theta_o)\tan\phi]-\frac{D}{r_o}-\frac{H}{r_o}(a_1\cot\beta_1+a_2\cot\beta_2) \tag{2}$$

$$\frac{H}{r_o}=\sin\theta_o\exp[(\theta_h-\theta_o)\tan\phi]-\sin\theta_o \tag{3}$$

$$\frac{N}{r_o}=\cos\phi\exp[(\frac{\pi}{2}+\phi-\theta_o)\tan\phi]-\sin\theta_o-\frac{H}{r_o} \tag{4}$$

where a_1, a_2, D and N are defined in Fig. 1 (a). The rate of external work done by the region AA' CB' B can be obtained from the algebraic summation of $\dot{W}_1-\dot{W}_2-\dot{W}_3-\dot{W}_4-\dot{W}_5$. Herein, $\dot{W}_1$, $\dot{W}_2$, $\dot{W}_3$, $\dot{W}_4$ and $\dot{W}_5$ represent the rates of external work done by the soil weight in the region OAB', OB' B, OCB, OA' C and OAA' respectively.

These expressions are

$$\dot{W}_1=\gamma\Omega r_o^3[\frac{1}{3(1+9\tan2\phi)}\{(3\tan\phi\cos\theta_h+\sin\theta_h)\exp[3(\theta_h-\theta_o)\tan\phi]-3\tan\phi\cos\theta_o-\sin\theta_o\}] \tag{5}$$

$$=\gamma\Omega r_o^3G_1$$

$$\dot{W}_2=\gamma r_o^3\Omega\frac{1}{6}\sin\theta_o\frac{L}{r_o}\{2\cos\theta_o-\frac{L}{r_o}\}$$

$$=\gamma r_o^3\Omega G_2 \tag{6}$$

$$\dot{W}_3=\gamma r_o^3\Omega[\frac{a_1}{3}\frac{H}{r_o}\{\cos^2\theta_o+\frac{L}{r_o}(\frac{L}{r_o}-2\cos\theta_o)+\sin\theta_o\cot\beta_1(\cos\theta_o-\frac{L}{r_o})-\frac{a_1}{2}\frac{H}{r_o}\cot\beta_1(\cos\theta_o-\frac{L}{r_0}+\sin\theta_o\cot\beta_1)\}]$$

$$=\gamma r_o^3\Omega G_3 \tag{7}$$

$$\dot{W}_4=\gamma r_o^3\Omega\frac{a_2}{3}\frac{H}{r_o}[(\cos^2\theta_h+\cot\beta_2\sin\theta_h\cos\theta_h)\exp[2(\theta_h-\theta_o)\tan\phi]+(\frac{D}{r_o}\cot\beta_2\sin\theta_h+\frac{a_2}{2}\frac{H}{r_o}\sin\theta h\cot\beta_2+2\frac{D}{r_o}\cos\theta_h+\frac{a_2}{2}\frac{H}{r_o}\cot\beta_2\cos\theta_h)\exp[(\theta_h-\theta_o)\tan\phi]+(\frac{D}{r_o})^2+\frac{a_2}{2}\frac{H}{r_o}\cot\beta_2(\frac{D}{r_o})]$$

$$=\gamma r_o^3\Omega G_4 \tag{8}$$

$$\dot{W}_5=\gamma r_o^3\Omega\frac{1}{6}\frac{D}{r_o}\sin\theta_h[\{2\cos\theta_h\exp[(\theta_h-\theta_o)\tan\phi]+\frac{D}{r_o}\}\exp[(\theta_h-\theta_o)\tan\phi]]$$

$$=\gamma r_o^3\Omega G_5 \tag{9}$$

Similarly, the rate of external work done by the inertia force on the soil weight can be found simple summation by $\dot{W}_6-\dot{W}_7-\dot{W}_8-\dot{W}_9-\dot{W}_{10}$ · Herein, $\dot{W}_6$, $\dot{W}_7$, $\dot{W}_8$, $\dot{W}_9$ and $\dot{W}_{10}$ represent the rates of external wopk done by the inertia force due to sliding soil weight in regions OAB', OB'B, OCB, OA' C and OAA', respectively.

These expressions are as follows

$$\dot{W}_6=K\ \gamma\ r_o^3\Omega\ [\frac{1}{3(1+9\tan 2\phi)}\ \{(3\tan\phi\sin\theta_h-\cos\theta_h)\exp\ [3(\theta_h-\theta_o)\tan\phi]$$

$$-3\tan\phi\sin\theta_o+\cos\theta_o\}]$$

$$=K\ \gamma\ r_o^3\Omega G_6 \tag{10}$$

$$\dot{W}_7=\frac{K\ \gamma\ r_o^3\Omega}{3}\ \{\frac{L}{r_o}\sin\theta_o\sin\theta_o\}$$

$$=K\ \gamma\ r_o^3\Omega_7 \tag{11}$$

$$\dot{W}_8=K\ \gamma\ r_o^3\Omega\ [\frac{a_1}{3}\frac{H}{r_o}\ \{\sin\theta_o+\frac{a_1}{2}(\frac{H}{r_o})\}\ (\cos\theta_o+\sin\theta_o\cos\beta_1-\frac{L}{r_o})]$$

$$=K\ \gamma\ r_o^3\Omega G_8 \tag{12}$$

$$\dot{W}_9=\frac{K\ \gamma\ r_o^3\Omega}{3}\ [\sin\theta_h\cos\theta_h(\sin\theta_o+\frac{H}{r_o})\exp\ [2(\theta_h-\theta_o)\tan\phi]$$

$$+\exp\ [(\theta_h-\theta_o)\tan\phi]\ [\sin\theta_h\frac{D}{r_o}(\sin\theta_o+\frac{H}{r_o})-\cos\theta_h\ \{\sin\theta_o+(a_2+1)\frac{H}{r_o}$$

$$+(\frac{a_2H}{r_o})^2\}]-\frac{D}{r_o}\ \{\sin\theta_o+(a_2+1)\frac{H}{r_o}+(\frac{a_2H}{r_o})^2\}-a_2\cot\beta_2\frac{H}{r_o}$$

$$\{\sin\theta_o+(1-a_2)\frac{H}{r_o}(\sin\theta_o+\frac{H}{r_o})]$$

$$=K\ \gamma\ r_o^3\Omega G_9 \tag{13}$$

$$\dot{W}_{10}=K\ \gamma\ r_o^3\Omega\ \{\frac{1}{3}\frac{D}{r_o}\sin^2\theta_h\exp\ [2(\theta_h-\theta_o)\tan\phi]\}$$

$$=K\ \gamma\ r_o^3\Omega G_{10} \tag{14}$$

The external rate of work due to surcharge boundary loads and its associated inertia force are found to be

due to surcharge

$$p\ r_o^2\Omega\{Lr_o(\cos\theta_o-\frac{L}{2r_o})\}=p\ r_o^2\Omega\ f_p \tag{15}$$

due to inertia force of the surcharge

$$xKp\ r_o^2\Omega\ \{\frac{L}{r_o}\sin\theta_o\}=p\ r_o^2\Omega\ f_q \tag{16}$$

The total rates of internal energy dissipation along the discontinuous log-spiral failure surface AB is found by multiplying the differential area $rd\theta/\cos\phi$ by c_i times the discontinuity in velocity, $V\cos\phi$, across the surface and integrating over the whole surface AB. Since the layered clays possess different values of c_i, the integration is therefore carried out into two parts.

$$\int_{\theta_o}^{\theta_h} c_i(V\cos\phi)\frac{\mathrm{rd}\,\theta}{\cos\phi} = \int_{\theta_o}^{\theta_h} (c_i)_I\, r_o\, v_o \exp[2(\theta-\theta_o)\tan\phi]\,d\theta + \int_{\theta_o}^{\theta_h} (c_i)_{II} r_o\, v_o \exp[2(\theta-\theta_o)\tan\phi]\,d\theta \tag{17}$$

The log-spiral angle, θ_m and the anisotropic angle, i are related from the geometric configuration shown in Figs. 1 (a)(b) as

$$\sin\theta_m \exp[\theta_m\tan\phi] = \sin\theta_h \exp[\theta_h\tan\phi] \tag{18}$$

Referring to equation (1) and the geometry of Fig. 1, $(c_i)_I$ and $(c_i)_{II}$ can be expressed as

in the region θ_o and θ_m

$$(c_i)_I = \{1+(\frac{1-k}{k})\cos^2 i\}\, c\,\{n_o + \frac{1-n_o}{\frac{H}{r_0}}(\sin\theta\exp[(\theta-\theta_0)\tan\phi]-\sin\theta_0)\} \tag{19}$$

in the region θ_m and θ_h

$$(c_i)_{II} = \{1+(\frac{1-k}{k})\cos^2 i\}\, c\,\{n_1 + \frac{n_2-n_1}{\frac{N}{r_0}}(\sin\theta\exp[\theta-\theta_0)\tan\phi] - \sin\theta_m\exp[(\theta_m-\theta_0)\tan\phi]\} \tag{20}$$

where $K=\frac{c_h}{c_v}$, $i=\theta+\Phi$, $\Phi=-(\frac{\pi}{2}+\phi-m)$ and

n_o, n_1 and n_2 are defined in Fig. 1 (c).

After integration and some simplifications, Eq. (17) reduces to

$$\int_{\theta_o}^{\theta_h} c_i(V\cos\phi)\frac{\mathrm{rd}\,\theta}{\cos\phi} = c\, r_o^2\, \Omega\, Q \tag{21}$$

in which

$$Q = Q_1 + Q_2 + Q_3 \tag{22}$$

The functions Q_1, Q_2 and Q_3 are

$$Q_1 = \frac{n_o}{\exp(2\theta_o\tan\phi)}\left|\psi+\left(\frac{1-k}{k}\right)\lambda\right|_{\theta_o}^{\theta_m} + \frac{n_1}{\exp(2\theta_o\tan\phi)}\left|\psi+\left(\frac{1-k}{k}\right)\lambda\right|_{\theta_m}^{\theta_h} \tag{23}$$

$$Q_2 = \frac{1-n_o}{\left(\frac{H}{r_o}\right)\exp(3\theta_o\tan\phi)}\left|\xi-\psi\sin\theta_o\exp[\theta_o\tan\phi] + \left(\frac{1-k}{k}\right)\{\rho-\lambda\sin\theta_o\exp[\theta_o\tan\phi]\right|_{\theta_o}^{\theta_m} \tag{24}$$

$$Q_3 = \frac{n_2-n_1}{\left(\frac{N}{r_o}\right)\exp(3\theta_o\tan\phi)}\left|\xi-\psi\sin\theta_m\exp[\theta_m\tan\phi] + \left(\frac{1-k}{k}\right)\{\rho-\lambda\sin\theta_m\exp[\theta_m\tan\phi]\right|_{\theta_m}^{\theta_n} \tag{25}$$

in which

$$\xi = \frac{(3\tan\phi\sin\theta-\cos\theta)}{1+9\tan^2\phi}\exp[3\theta\tan\phi] \tag{26}$$

$$\psi = \frac{\exp[2\theta\tan\phi]}{2\tan\phi} \tag{27}$$

$$\rho = \frac{\exp[3\theta\tan\phi]}{2}\left\{\frac{3\tan\phi\sin\theta-\cos\theta}{1+9\tan^2\phi}+\cos 2\Phi\left\{\frac{\tan\phi\sin 3\theta-\cos 3\theta}{6(1+\tan^2\phi)}\right.\right.$$
$$\left.\left.+\frac{\cos\theta 3\tan\theta\sin\theta}{2(1+9\tan^2\phi)}\right\}-\sin 2\Phi\left\{\frac{\sin\theta+3\tan\phi\cos\theta}{2(1+9\tan^2\phi)}-\frac{\sin\theta+\tan\phi\cos 3\theta}{6(1+\tan^2\phi)}\right\}\right. \tag{28}$$

$$\lambda = \frac{\exp[2\theta\tan\phi]}{2}\left\{\frac{\exp[2\theta\tan\phi]}{4\tan\phi}+\frac{\exp[2\theta\tan\phi}{2}\right.$$
$$\left.\cdot\left\{\frac{\cos 2\Phi(\tan\phi\cos 2\theta+\sin 2\theta)}{2(1+\tan^2\phi)}-\frac{\sin 2\Phi(\tan\phi\sin 2\theta-\cos 2\theta)}{2(1+\tan^2\phi)}\right\}\right. \tag{29}$$

By equating the total rates of external work, Eq. (5) to (16) to the total rate of internal energy dissipation, Eq. (21), we obtain

$$K=F\left(\theta_o, \theta_h, \frac{D}{r_o}\right)=\frac{c(Q_1+Q_2+Q_3)-\gamma r_o(G_1-G_2-G_3-G_4-G_5)-pf_p}{\gamma r_o(G_6-G_7-G_8-G_9-G_{10})+xpf_q} \tag{30}$$

The function $F\left(\theta_o, \theta_h, \frac{D}{r_o}\right)$ has a minimum value and, thus, indicates a least upper bound, when θ_o, θ_h, and $\frac{D}{r_o}$ satisfy the following conditions.

$$\frac{\partial K}{\partial\theta_o}=0\ ;\ \frac{\partial K}{\partial\theta_h}=0 \text{ and } \frac{\partial K}{\partial D/r_o}=0 \tag{31}$$

Thus, the yield acceleration factor, K_c is denoted as

$$K_c=\text{Min. } F(\theta_o, \theta_h, D/r_o) \tag{32}$$

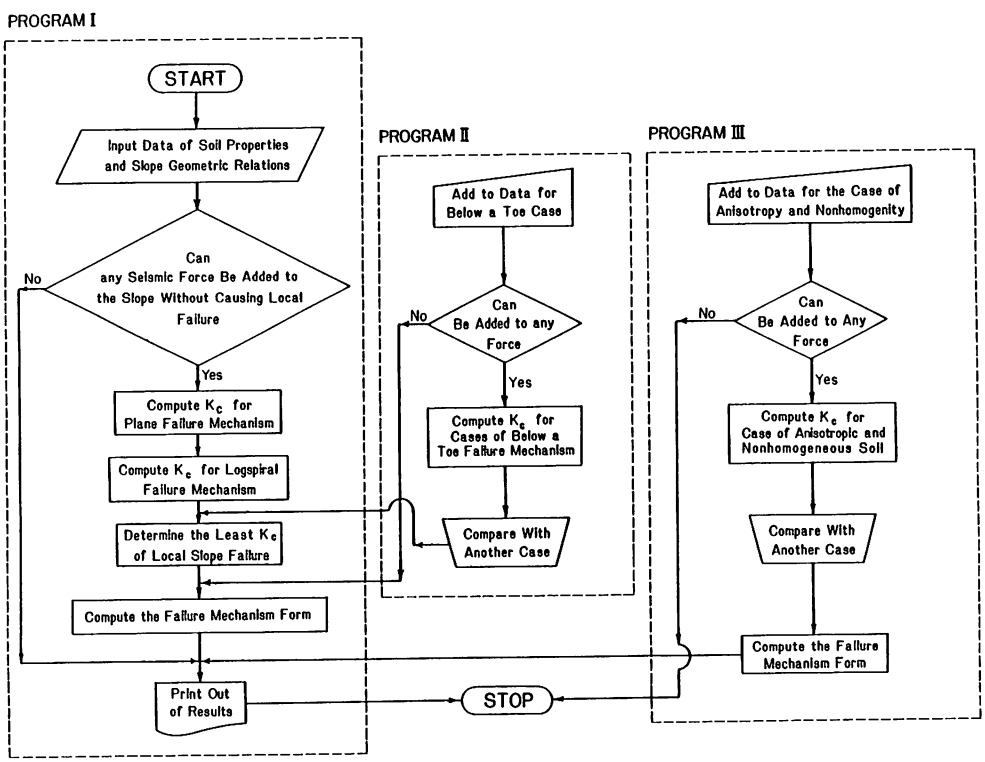

Fig. 3 Flow Chart

III. Flow Chart

The flow chart of the computer is given in Fig. 3 In the following, a brief explanation of these logical steps is given. These steps are summarized in the following sequence :

(1) Read input data from free format I , the read-in sequence and explanation of input Datas are shown in the program listing.

(2) Before searching K_c of local failure, check if horizontal inertia force can be imposed. If it is possible, it means that the slope has already failed before imposing any seismic force.

(3) Compute K_c for translational plane failure mechanism using OPT which is a package of FORTRAN IV subroutine (Gabriele and Pagsdell 1976) and also implements the generalized reduced gradient method for the solution of the constrained nonlinear programming problem.

(4) Compute K_c for the rotational log-spiral failure mechanism using OPT.

(5) The critical value K_c corresponding to the log-spiral mechanism is smaller than that of plane failure mechanism. However, a comparison between the two yield acceleration factors corresponding to plane and log-spiral failure surface is still necessary.

Case 1 : Log-spiral failure surface passing below the toe for homogeneous and isotropic slopes. Details of this are in Appendix C. Logical steps are of course identical to that described above except the expressions used in the program OPT.

Case 2 : Log-spiral failure surface for nonhomogeneous and anisotropic slopes. The steps are the same as above cases.

IV. NUMERICAL RESULTS

Here, as in nonhomogeneous and isotropic case, the numerical results of K_c values are obtained by the CDC 6600 and CDC 6500 digital computers. The optimization technique reported by Sigel (1978) is used to minimize the function of Eq. (32) without calculating the derivatives. The results are

Table 1 Comparison of Critical Height : H_c for Anisotropic Soil with Constant Shear Strength

Slope Angle (Degree) β	Anisotropy Factor k	Curved Failure Surface		
		Limit :1 Equilibrium ϕ Circle*	Limit :2 Analysis Log Spiral	ratio of 1 / 2
90	1.0	95.75	110.57	0.870
	0.9	--	--	--
	0.8	--	--	--
	0.7	--	--	--
	0.6	--	--	--
	0.5	--	--	--
70	1.0	119.75	136.62	0.877
	0.9	118.00	132.36	0.892
	0.8	116.25	128.14	0.907
	0.7	114.50	123.89	0.924
	0.6	112.25	119.12	0.942
	0.5	110.25	114.92	0.960
50	1.0	142.00	142.00	1.000
	0.9	138.50	137.50	1.007
	0.8	133.75	129.40	1.034
	0.7	129.75	125.50	1.054
	0.6	127.25	120.75	1.054
	0.5	121.25	116.50	1.041

*Lo (1965)

Table 2 Comparison of Critical Height : H_c for Anisotropic Soil with Shear Strength Increasing Linearly with Depth

Slope Angle (Degree) β	Anistropy Factor k	Curved Failure Surface		
		Limit :1 Equilibrium ϕ Circle*	Limit :2 Analysis Log Spiral	ratio of 1 / 2
90	1.0	50.00	60.97	0.820
	0.9	50.00	60.45	0.827
	0.8	50.00	60.30	0.829
	0.7	50.00	59.40	0.842
	0.6	50.00	58.85	0.850
	0.5	50.00	58.35	0.857
70	1.0	69.25	72.10	0.961
	0.9	68.25	72.06	0.947
	0.8	67.25	70.77	0.950
	0.7	66.25	70.40	0.941
	0.6	65.25	70.20	0.930
	0.5	62.50	68.68	0.910
50	1.0	94.50	103.70	0.911
	0.9	91.50	100.50	0.911
	0.8	89.00	98.00	0.908
	0.7	86.25	95.40	0.904
	0.6	82.75	92.40	0.896
	0.5	79.25	89.50	0.886
30	1.0	137.50	135.50	1.015
	0.9	--	--	--
	0.8	125.00	127.00	0.984
	0.7	--	--	--
	0.6	--	--	--
	0.5	104.50	114.00	0.917

*Lo (1965)

Table 3 Yield Acceleration Factor K_c with constant stability number N_s and surcharge P

Anisotropy factor k	p = 0 x = 0	p = 120psf x = 0	p = 120 psf x = 0.5
1.0	0.477	0.455	0.450
0.9	0.457	0.436	0.431
0.8	0.437	0.417	0.413
0.7	0.416	0.399	0.394
0.6	0.396	0.380	0.376
0.5	0.377	0.361	0.357

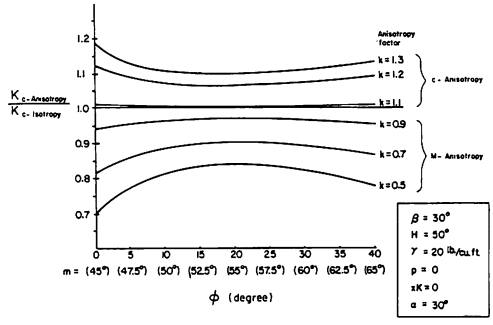

Fig. 4 Variation K_c, anisotropy vs K_c, isotropy Corresponding to Φ

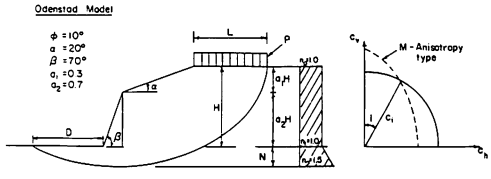

Table 4 Anisotropic but Homogeneous Soil : with constant C_v (Φ=constant, $\alpha=\beta$)

Taylor Model

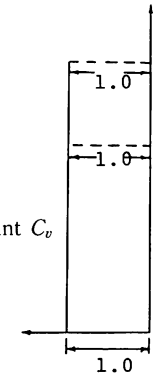

Friction Angle (degrees) φ	Anisotropy Factor k	Slope Angle β	Yield Acceleration Factor: K_c (degrees) 30	(degrees) 50	(degrees) 70	(degrees) 90
C-Anisotropy type	1.3		0.290	0.285	0.282	0.280
	1.2		0.275	0.270	0.268	0.266
	1.1		0.260	0.256	0.253	0.252
0.0	1.0		0.246	0.241	0.239	0.237
(m=45°)	0.9		0.231	0.227	0.225	0.223
	0.8		0.216	0.212	0.211	0.209
M-anisotropy type	0.7		0.201	0.198	0.196	0.195
	0.6		0.187	0.184	0.182	0.181
	0.5		0.172	0.169	0.168	0.167
C-Anisotropy type	1.3		0.361	0.356	0.354	0.352
	1.2		0.346	0.342	0.339	0.337
	1.1		0.331	0.327	0.325	0.323
5.0	1.0		0.316	0.312	0.310	0.309
(m=47.5°)	0.9		0.301	0.297	0.296	0.294
	0.8		0.286	0.283	0.281	0.280
M-Anisotropy type	0.7		0.271	0.268	0.267	0.266
	0.6		0.256	0.253	0.252	0.251
	0.5		0.240	0.239	0.238	0.237
C-Anisotropy type	1.3		0.459	0.454	0.451	0.449
	1.2		0.433	0.438	0.435	0.434
	1.1		0.432	0.422	0.420	0.418
	1.0		0.411	0.407	0.405	0.403
10.0	0.9		0.394	0.391	0.389	0.388
(m=50°)	0.8		0.378	0.375	0.374	0.373
M-Anisotropy type	0.7		0.362	0.359	0.358	0.357
	0.6		0.346	0.344	0.343	0.342
	0.5		0.329	0.328	0.327	0.326
C-Anisotropy type	1.3		0.739	0.729	0.725	0.721
	1.2		0.717	0.707	0.704	0.701
	1.1		0.695	0.686	0.683	0.680
	1.0		0.673	0.666	0.662	0.660
20.0	0.9		0.651	0.645	0.641	0.639
(m=60°)	0.8		0.629	0.623	0.621	0.619
M-Anisotropy type	0.7		0.607	0.602	0.600	0.598
	0.6		0.585	0.581	0.579	0.578
	0.5		0.562	0.560	0.558	0.557

Table 5 Anisotropic and Nonhomogeneous Soil : C_v Increasing Linearly with Depth

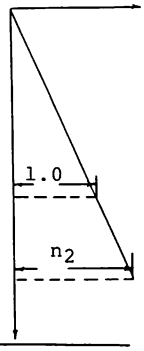

Gibson & Morgenstern Model

Friction Angle (degree) φ	Anisotropy Factor k	Yield Accelaration Factor: K_c Slope Angle (degree) β: 30	Slope Angle (degree) 50	Slope Angle (degree) 70	Slope Angle (degree) 90
0.0 (m=45°)	1.0	0.231	0.227	0.226	0.224
	0.9	0.216	0.213	0.211	0.210
	0.8	0.201	0.199	0.197	0.196
	0.7	0.186	0.184	0.183	0.182
	0.6	0.172	0.170	0.169	0.168
	0.5	0.157	0.155	0.155	0.154
5.0 (m=47.5°)	1.0	0.303	0.300	0.299	0.298
	0.9	0.288	0.286	0.284	0.283
	0.8	0.273	0.271	0.270	0.269
	0.7	0.258	0.256	0.255	0.255
	0.6	0.243	0.242	0.241	0.241
	0.5	0.228	0.227	0.227	0.226
10.0 (m=50°)	1.0	0.399	0.396	0.394	0.393
	0.9	0.383	0.380	0.379	0.378
	0.8	0.367	0.365	0.364	0.363
	0.7	0.350	0.349	0.348	0.348
	0.6	0.344	0.333	0.332	0.332
	0.5	0.318	0.318	0.317	0.317
20.0 (m=60°)	1.0	0.659	0.653	0.650	0.648
	0.9	--	0.632	0.629	0.628
	0.8	--	0.611	0.609	0.608
	0.7	--	0.590	0.588	0.587
	0.6	--	0.569	0.568	0.567
	0.5	--	0.548	0.547	0.547

Table 6 Anisotropic and Nonhomogeneous Soil : C_v Increasing with Depth (Φ=constant, $\alpha \neq \beta$)

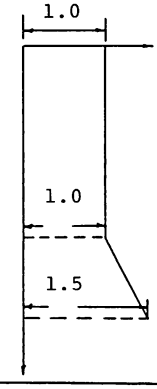

Odenstad Model

Friction Angle (degrees) φ	Anisotropy Factor k	Yield Acceleration Factor: K_c Slope Angle (degrees) β: 30	Slope Angle (degrees) 50	Slope Angle (degrees) 70	Slope Angle (degrees) 90
0.0 (m=45°)	1.0	0.329	0.323	0.320	0.318
	0.9	0.311	0.305	0.302	0.300
	0.8	0.293	0.287	0.284	0.282
	0.7	0.274	0.269	0.266	0.264
	0.6	0.255	0.250	0.248	0.246
	0.5	0.237	0.232	0.230	0.228
5.0 (m=47.5°)	1.0	0.395	0.389	0.386	0.383
	0.9	0.376	0.370	0.367	0.365
	0.8	0.356	0.351	0.349	0.347
	0.7	0.337	0.332	0.330	0.328
	0.6	0.318	0.314	0.311	0.310
	0.5	0.299	0.295	0.293	0.292
10.0 (m=50°)	1.0	0.486	0.480	0.477	0.474
	0.9	0.465	0.460	0.457	0.455
	0.8	0.445	0.439	0.437	0.435
	0.7	0.424	0.419	0.416	0.415
	0.6	0.403	0.399	0.396	0.395
	0.5	0.382	0.379	0.377	0.376
20.0 (m=60°)	1.0	0.741	0.732	0.727	0.724
	0.9	0.713	0.705	0.701	0.698
	0.8	0.686	0.678	0.675	0.672
	0.7	0.658	0.652	0.648	0.646
	0.6	0.631	0.625	0.622	0.620
	0.5	0.603	0.598	0.595	0.593

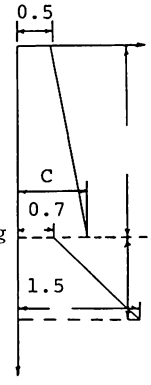

Table 7 Anisotropic and Nonhomogeneous Soil : C_v Increasing Linearly with Depth (Φ=constant, $\alpha=\beta$)

Reddy & Srinivason Model

Friction Angle (degrees) ϕ	Anisotropy Factor k	Yield Acceleration Factor: K_c Slope Angle (degrees) β: 30	Slope Angle (degrees) 50	Slope Angle (degrees) 70	Slope Angle (degrees) 90
0.0 (m=45°)	1.0	0.304	0.298	0.295	0.293
	0.9	0.286	0.281	0.278	0.276
	0.8	0.268	0.263	0.261	0.259
	0.7	0.250	0.245	0.243	0.242
	0.6	0.232	0.228	0.226	0.225
	0.5	0.213	0.210	0.209	0.207
5.0 (m=47.5°)	1.0	0.372	0.368	0.364	0.362
	0.9	0.354	0.350	0.347	0.345
	0.8	0.335	0.331	0.329	0.327
	0.7	0.317	0.313	0.311	0.310
	0.6	0.298	0.295	0.293	0.292
	0.5	0.280	0.277	0.276	0.275
10.0 (m=50°)	1.0	0.467	0.461	0.459	0.456
	0.9	0.447	0.442	0.440	0.438
	0.8	0.428	0.423	0.421	0.419
	0.7	0.409	0.404	0.402	0.401
	0.6	0.390	0.385	0.383	0.382
	0.5	0.369	0.365	0.364	0.363
20.0 (m=60°)	1.0	0.739	0.730	0.725	0.722
	0.9	0.712	0.704	0.700	0.697
	0.8	0.685	0.678	0.674	0.672
	0.7	0.658	0.652	0.649	0.647
	0.6	0.631	0.626	0.624	0.622
	0.5	0.605	0.600	0.598	0.597

summarized in Tables 1 to 7 and Fig. 4 Some of the solutions are compared in Tables 1 and 2 with the existing limit equilibrium solutions.

(1) Table 1 shows a comparison of critical heights obtained by the limit equilibrium method and by the present limit analysis for anisotropic slope with constant shear strength (Lo, 1965). Here, as in Lo's work, the value of m is taken to be 55° and the values of friction angle, ϕ and acceleration K_c are put nearly equal to zero so that the statical log-spiral failure surface reduces to the circular one. Generally speaking, both results are in good agreement.

(2) Table 2 compares the cases of anisotorpic slope with shear strength increasing linearly with depth. (Fig. 2, b). In this way, the critical height H_c can be compared with those obtained previously by Lo (1965) using the limit equilibrium method. A good agreement is again observed.

(3) Figure 4 illustrates graphically the K_c values of anisotropy case normalized by the corresponding K_c values of isotropy case with C-anisotropy type (or $k>1$) and M-anisotropy type (or $K<1$)(Lo, 1965).

(4) Some typical results for the yield acceleration K_c corresponding to the general case of nonhomogeneous and anisotropic soil are tabulated in Tables 4 to 7. These include (see Fig. 2)

Table 3 —Yield Acceleration Factor k_c with constant Stability Number N_s and surcharge p

Table 4 —Taylor model (1948)

Table 5 —Gibson and Morgenstern model (1962)

Table 6 —Odenstad model (1963)

Table 7 —Reddy and Srinivason model (1967)

where the angle m between the failure plane and major principal plane as shown in Fig. 1 (a) is taken to be $\frac{\pi}{4}+\frac{\phi}{2}$.

V. Summary and Conclusions

The purpose of this study is to establish a practical approach to obtain effectively the slope stability solutions under earthquake loading condition. To this end, the upper bound technique of limit analysis is applied to obtain the yield acceleration factor for two cases of clay slopes : (1) homogeneous but anisotropic slopes (2) nonhomogeneous and anisotropic slopes. For practical purpose, we adopt the pseudo-static approach and not a dynamic analysis. The formulation of the problem is seen to be rather straightforward and simple. The numerical results for the special cases are found to be in good agreement with the existing limit equilibrium solutions.

It can therefore be concluded that the upper bound technique of limit analysis provides a convenient and effective method for the analysis for seismic stability of earth slopes. In a subsequent work we will report on the assessment and evaluation of seismic displacements considering the potential of liquefaction effects for anisotropic, non-homogeneous clay. slopes. These studies are considered to be necessary for a better definition of the failure of slopes under earthquake loading conditions.

Reference

1. Chen, W. F., "Limit Analysis and Soil Plasticity" Elsevier Scientific Publishing Co., Amsterdam, The Netherland, 1975.

2. Chen, W. F., "Limit Analysis of Stability of Slopes", Journal of the soil Mechanics and Foundation Division, ASCE, Vol. 97, No. SMI, January, 1971, pp. 19−26.

3. Chen, W. F. and Sawada, T., "Earthquake-Induced Slope Failure in Nonhomogeneous, Anisotropic Soils", Soils and Foundations, The Jakanese Society of Soil Mechanics and Foundations Fngineering, Vol. 23, No.2, June, 1983, pp.125−139.

4. Sawada, T., Nomachi, S. G. and Chen, W. F., "Seismic Stability of Nonhomogeneous, Anisotropic Slopes, "Speciality Conference, ASCE, EMD, Vol. II, May, 1983, pp.1009−1013.

5. Gabriele, G. A. and Pagsdell, K. M., "OPT : A Nonlinear Programming Code in Fortran-IV User's Manual", The Modern Design Series, Purdue Research Foundation C, School of Mechanical Engineering, Purdue University, West Lafayette, IN 1976.

6. Gibson, R. F. and Morgenstern, N., "A Note on the stability of cutting in Normally Consolidated clays". Geotechnique, institution of Civ. Engrs., London, England, Vol. 12, No. 3, 1962, pp. 212−216.

7. Lo, K. Y., "Stability of Slopes in Anisotropic Soils", Journal of the Soil Mechanics and Foundation Division, ASCE, Vol. 91, No. SM4, July, 1965, pp. 85−106.

8. Odenstad, S., "Correspondence", Geotechnique, Vol. 13, No. 2, 1963, pp. 166−170.

9. Reddy, A. S. and Srinivason, R. J., "Bearing Capacity of Footing on Layered Clays", Journal of the Soil Mechanics and Foundations Division, ASCE, Vol. 93, No. SM2, March, 1967, pp. 83−98.

10. Sigel, R. A., "STABL user Manual", Joint Highway Research Project, JHRP−75−9, Schook of Civil Engineering, Purdue University, West Lafayette, IN 1978.

11. Taylor, D. W., "Fundamental of Soil Mechanics", John Wiley and Sons, New York, N. Y., 1948.

(昭和58年11月30日受理)